Available online at www.sciencedirect.com
SCIENCE DIRECT®
International Journal of Thermal Sciences 45 (2006) 760–773
International Journal of Thermal Sciences
www.elsevier.com/locate/ijts

Unsteady methods (URANS and LES) for simulation of combustion systems ☆

A. Sadiki *, A. Maltsev, B. Wegner, F. Flemming, A. Kempf, J. Janicka

Institute of Energy and Power Plant Technology, Department of Mechanical Engineering, Technical University of Darmstadt, Petersenstr. 30, 64287 Darmstadt, Germany

Received 25 October 2004; received in revised form 26 October 2005; accepted 5 November 2005

Available online 27 December 2005

Abstract

A great variety of flows in practical engineering applications are inherently unsteady, and virtually all of Newtonian fluid flows in nature are turbulent. In order to better capture the dynamics of such complex flows, it is appropriate to use unsteady methods. The present overview is confined to single-phase turbulent flows. The first part provides an evaluation of the performance of the unsteady RANS (URANS) method. It could be confirmed that the U-RANS method employing a full Reynolds stress model is able to capture unsteady phenomena, such as precessing vortex core phenomenon both qualitatively and in parts also quantitatively. In the second part, some important features of combustion LES are recollected and some results for flames, that were already computed by RANS-based methods in the literature, are presented. Thereby a flamelet approach is used to relate the filtered mixture fraction to density, temperature and species concentrations. It is shown that LES is able to deliver good results very close to measured data, where the flow is governed by large, turbulent structures. Flamelet chemistry appears well able to reproduce experimental data for species, in particular with regard to kinetic effects prediction, whereas equilibrium chemistry strongly deviates. However, a good predictability could be achieved when appropriate choice of boundary and inflow conditions is made.

Keywords: Unsteady methods; URANS; LES; Turbulent flows; Turbulent combustion systems

1. Introduction

A great variety of Newtonian flows with importance to industrial applications are turbulent and involve complex physical phenomena, such as combustion and other chemical reactions, multiphase and multicomponent interactions as well as heat transfer problems [1–55,57–60]. Besides recent advancements in measurement techniques suitable for a properly experimental description of such flows [31,41], the development of computers and application-oriented numerical methods, computational and programming techniques, data pre- and post-processing, grid generation and graphical representation has reached a standard of reliability and accuracy sufficient to make the Computational Fluid Dynamics (CFD) a useful design tool in many fields of engineering [14]. For the flow simulation, stationary RANS- (here Reynolds-averaging based numerical simulation) type calculations are state of the art in engineering practice. This is mostly motivated by reasonable computational costs required by this method. In RANS, one generally splits the flow variables into one mean part and one turbulent part, so that unclosed terms appear in the thermo-mechanical governing transport equations. These terms are usually modeled by means of turbulence models at the first or second order closure level. Although the superiority of the differential second-moment turbulence closure models (DSM) is well recognized, its slow adoption by the CFD community illustrates a higher degree of persisting numerical difficulties and uncertainties in modeling some terms, such as pressure-scrambling [14]. In complex flows involving heat and mass transfer as well as combustion, for example, the coupling between the Reynolds stress (tensor) and scalar flux (vector) fields and mean flow, the number of addi-

☆ A preliminary version of this paper was presented at CHT-04: An ICHMT International Symposium on Advances in Computational Heat Transfer, April 2004, G. de Vahl Davis and E. Leonardi (Eds.), CD-ROM Proceedings, ISBN 1-5670-174-2, Begell House, New York, 2004.

* Corresponding author. Tel.: +49 (0)6151 16 2757; fax: +49 (0)6151 16 6555.

E-mail address: sadiki@ekt.tu-darmstadt.de (A. Sadiki).

1290-0729/$ – see front matter
doi:10.1016/j.ijthermalsci.2005.11.001

tional transport equations to be solved, increase dramatically. This complexity, together with equation stiffness, reduces the attractiveness of the DSM. Explicit algebraic Reynolds stress (Scalar flux) modeling seems to offer a compromising route, accounting for most of the physical sounds included in DSM while keeping the computational efficiency and robustness of the two-equations approach. For a recent review, see e.g. Durbin [3,12,14].

Experience reveals that many types of practical turbulent flows are configuration dependent and evolve in an unsteady manner making steady state computations, at best, an approximation. Direct numerical simulations (DNS) allow in fact to resolve all scale structures, but are computationally time consuming and remain limited to low Reynolds numbers (see e.g. [46]). In order to better capture the dynamics of turbulent complex flows using feasible computational costs, unsteady RANS (URANS) and large eddy simulation (LES) emerge as the only realistic alternatives. As pointed out in [7,56], these methodologies produce different representations at different levels of resolution.

The simulation of only the largest scales of turbulence, generally called Large Eddy Simulation, is performable for configurations with higher Reynolds numbers [1,2,5–10]. The formulation of LES equations and models leads to several LES approaches within the framework of turbulence simulation research. The simple approach is a no-model implementation [8], in which numerical dissipation plays the role of the model. In the classical approach for LES the governing equations (the continuity equation, the Navier–Stokes equations, the energy equation, etc.) are filtered to separate the large-scale and small-scale turbulence (e.g. [1,2,4]). The large-scale turbulence is solved for by the discretized equations whereas the small-scale turbulence is modeled through the subgrid scales (SGS) models. Different SGS models in non-reacting flows have been developed. They consist mainly of gradient assumption based models, so-called linear eddy-viscosity models using constant or dynamically determined [4] model coefficient. One-equation model or second order model approach can also be mentioned. For recent reviews, see, e.g., Lesieur and Metais [5] or Sagaut [6]. Since turbulence is three-dimensional and unsteady, it means that LES must always be carried out as 3D, unsteady simulations. To perform an accurate LES, a very fine mesh must be used. This causes problems, for example, near walls where no large scales are present. LES is therefore expected to be very good for flow systems, where the flow is governed by large, turbulent structures, which can be captured by a fairly coarse mesh. However, if attached boundary layers are important, LES will probably give very poor predictions in these regions, unless very fine grids are used [10,12]. In this case, a variant of the RANS method called Unsteady RANS (URANS) approach, in which the Reynolds averaged equations and models are solved in three-dimensions with time dependence [11–13] is expected to be reliable than classical LES. It will require significantly less computational costs. In fact, by definition of time-averaging (or ensemble averaging under ergodic hypothesis) in RANS-context, all scales smaller than a characteristic time T are modeled by the closure and the only unsteadiness allowed is at time scales larger than T. To apply RANS models, originally developed for steady state cases, to unsteady flow applications, T has to be considered smaller than some of the turbulent time scales. In contrast to this, another unsteady RANS approach requires that the turbulence model be developed using a methodology that takes into account the interaction between the unresolved and resolved scales. This approach that employs a "time-accurate" RANS turbulence closure is denoted as very large-eddy simulation (VLES) (see in [7]). It is also known as a kind of hybrid RANS/LES. The basic idea behind VLES is to resolve only very large coherent, or deterministic structures and model the remaining part, the incoherent random fluctuations. However, this form of RANS model is not related to the size of the numerical mesh. The solution of the resolved part of the spectrum can follow the traditional LES practice using grid size as a basis for defining the filter, or solve ensemble or conditionally averaged governing equations [60]. An example may be the two-equations model based on the renormalization group theory (RNG).

With regard to combustion, two major objectives in modern design of technical combustion systems, in which heat and mass transfer play a central role, are optimization of combustion efficiency and reduction of pollutants, such as nitric oxides or carbon monoxide. In order to meet these requirements, designers are limited by current modeling approaches. Nowadays, the importance of large scale structures of the flow in scalar mixing and combustion is well accepted: turbulent eddies can really wrinkle the flame and even quench it; eddies improve heat transfer and mixing of species which contribute to increase the efficiency of technical combustion devices. Numerical models for reacting flows capable of providing the necessary information must therefore be able to predict the highly unsteady behavior, in particular that associated with turbulence-chemistry interactions. For this purpose, a complete model formulation has to contain physics-preserving turbulence/mixing closures, an appropriate combustion model along with a model accounting for turbulence-chemistry interactions and probable radiation processes [15–41,44,47,55,57]. In this regard, it must be mentioned that chemical reactions, in non-premixed flames for example, occur only by molecular mixing of fuel and oxidizer, which in general occurs on the dissipative turbulent scales. Thus, the combustion process occurs essentially at the smallest scales of the sub-filter level, which has to be modeled in LES. As in averaged governing transport equations in URANS-techniques [53,55], additional closure problems arise as well from combustion related terms in the filtered governing transport equations used in LES.

Common in all the applications of LES to non-premixed combustion is the use of the gradient diffusion assumption to model the species transport terms due to turbulence. Use of this type of assumption for reactive species is questionable and even dubious [9,47]. An alternative subgrid modeling approach which avoids this assumption has been proposed in [25] by Kerstein and co-workers. In this approach, all relevant length scales are resolved in one dimension. Molecular diffusion is treated explicitly and subgrid stirring is modeled by a stochastic rearrangement process applied to a scalar field along the lin-

ear domain [48]. This process which involves a Monte Carlo simulation at each grid cell of an LES renders this method computationally very intensive. A review of existing scalar transport modeling strategies can be found in [49].

Proper treatment of the filtered reaction source term comprises most of the difficulty in LES subgrid modeling. Apart from the first LES in which the filtered chemical source terms were approximated in terms of the LES resolved field only and the effect of turbulent subgrid fluctuations was neglected [15] and an extension of the eddy-dissipation model of Magnussen and Hjertager to LES [16], the two combustion models that are mainly applied are the probability density function (PDF) transport equation approach and the flamelet approach. The derivation of the large eddy probability density function of the various chemical species has been performed in [16,35]. Although this approach is important for theoretical considerations, it appears to be computationally intensive. For non-premixed combustion, a functional form for the large eddy probability density function of a mixture has been postulated along with a laminar flamelet approach to subgrid-scale chemistry in turbulent flows in [17–21,26–29,32–34,51]. For the case of equilibrium chemistry, see e.g. [17,19,20]. The common idea behind flamelet models is to decouple the numerical simulation of the turbulent flow and mixture fields from the solution of the chemistry. Rather than using steady state flamelets, extension to unsteady flamelets approach has been suggested in [26,27]. In this model, unsteady flamelets are solved, which are introduced at the inlet nozzle and assumed to be transported downstream, essentially by convective transport. The time coordinate in the flamelet equations then becomes a Lagrangian-like time. The scalar dissipation rate appearing as a parameter is modeled by its conditional average over cross-sectional planes perpendicular to the jet axis. To account for probable local inhomogeneities of the scalar dissipation rate, the concept has been currently extended in [52]. In fact, many recent works dealing with combustion LES focus on the applicability of RANS-like combustion models in LES. The proposed models can be classified in five categories: direct method, see in [15,16,44], linear eddy model [24,25], transported pdf method (e.g. [16,35]) and conserved scalar method (e.g. [17–21,26–29,32–34,51,52]).

In addition to the turbulent species transport and to the filtered source terms, subgrid models for the temperature-species correlations arising in the state equations need to be formulated. However, their modeling has till now received little or no attention. As pointed out in [25] these correlations are generally neglected although they are expected to be non-negligeable for simulations with high heat release.

So far, numerical investigations based on URANS and LES have been reported both for non-premixed and premixed combustion. With regard to the latter, premixed turbulent combustion occurs in technical devices often in thin flame fronts [40]. The propagation of these fronts, and hence, for instance, the heat release, are governed by the interaction of transport processes and chemistry within the front. For premixed flame simulations, the use of an equation (G-equation in [22,33,39, 40] or c-equation in [30,38]) to track the propagation of a thin flame front is therefore state of the art. Concepts including the linear eddy model (LEM) [48] or the thickened flame assumption [36] must also be mentioned.

As far as complex reacting flows in practical devices are concerned, subgrid combustion models should be able to predict without ad hoc model adjustments premixed, non-premixed and partially premixed combustion often occurring simultaneously. However, only a few works focus on partially premixed configurations (e.g. [38,39]).

The present overview is confined to single-phase turbulent flows and discuses some basic issues related to unsteady modeling methods. The first part of this paper provides an evaluation of the performance of the unsteady RANS (U-RANS) method in a comparative manner to LES and experimental data. In the second part, some important features of combustion LES are summarized and some results based on the conserved scalar method in connection with the concept of sub-grid scale pdf are presented. In the following section the governing equations used are briefly presented along with the U-RANS and LES methodologies and the numerical scheme. The next section specifies the configurations under investigation, the grid, the boundary conditions and some results in two steps. First, a detailed description of the flow topologies of a swirled isothermal flow configuration using U-RANS is given in comparison to LES and experimental data. Secondly, two flame configurations, that were already investigated by means of RANS-based simulations, are chosen. As these flames do not exhibit particular unsteady or periodic phenomena, such as coherent or deterministic structures, only combustion LES computations are highlighted here. In the conclusion, the performance and limitations of unsteady methods for simulation of combustion systems are afterwards evaluated.

2. Governing equations, modeling and computational method

It is important to note that in these unsteady techniques one deals with the same form of governing equations, of course with different meaning of variables. This makes it convenient to use the same computational code and similar numerics and if necessary to combine the two approaches, as pointed out in [60]. For both the U-RANS and the LES approach under study the time dependent three dimensional (averaged/filtered) continuity and Navier–Stokes equations, as already presented in [19–21], are considered for describing the flow field in variable density fluids. In this section, we restrict to the methodologies used for the applications to be presented in the next section.

2.1. U-RANS modeling

The Reynolds/Favre averaged equations and models are solved in three-dimensions with time dependence [3,11–13] for non-reacting flows. For reacting case, the reader may refer to [53,55]. To close the governing equations, a standard k–epsilon-model and a second-order closure (DSM) chosen for its well-known capability to well predict complex flows have been used. For the DSM model the linear model of Jones and Musonge (see in [12]) was applied. For near wall treatment

the logarithmic law of the wall has been employed in conjunction with an explicit setting of the Reynolds stress anisotropy at the wall based on experimental data. Other DSM were also tried out in the course of this investigation, but no systematic study of model behavior has been performed though yet. The governing equations were discretized on a block-structured boundary-fitted collocated grid following the finite-volume approach. Spatial discretizations are 2nd order with a flux blending technique for the convective terms. The solution is forwarded in time using the 2nd order accurate implicit Crank–Nicolson scheme. A SIMPLE type pressure correction method is used for pressure-velocity coupling. The resulting set of linear equations are solved iteratively.

For the U-RANS computations, a flux blending parameter $\alpha = 0.5$ (i.e. 50% 1st order upwind differencing) was first used to ensure stability of simulations. After the simulations had evolved, the flux blending parameter could be increased up to $\alpha = 0.9$, thus reducing the upwind contribution to 10%. Throughout the paper all the LES used for comparison with URANS were run with almost pure central differencing ($\alpha = 0.95$) using the same CFD code. The time step width was chosen to give a CFL number of the order of 5 for the U-RANS. For the LES the time step width was smaller by a factor of 10 to resolve all turbulent fluctuations down to the grid-scale eddies.

2.2. LES modeling

In this paper, focus is made on the classical approach for LES. The governing equations (the continuity equation, the Navier–Stokes equations, the energy equation, etc.) are filtered to separate the large-scale and small-scale turbulence. The large-scale turbulence is solved for by the discretized equations whereas the small-scale turbulence is modeled through the subgrid scales (SGS) models. Different aspects related to the filtering techniques are treated in a comprehensive manner in [1,2,4–7,56]. For the non-reacting case, a Smagorinsky-model with dynamic procedure according to [4] was used to determine the subgrid scale stresses. In order to stabilize the model, the modification proposed in [50] is applied. In addition a clipping approach will reset negative Germano coefficient to zero to avoid destabilizing values of the model coefficient. The filtering operation is performed implicitly by means of the finite-volume discretization. No special wall-treatment is included in the subgrid-scale model. We rather rely on the ability of the dynamic procedure to capture the correct asymptotic behavior of the turbulent flow when approaching the wall, see e.g. [4,5].

For reacting cases, we use the conserved scalar formulation. It is then assumed that the chemical state and thereby the species mass fractions can be related to a conserved scalar, the mixture fraction, which sub-grid scale pdf is presumed to follow a Beta-function distribution. In numerical method, fluctuations of density in space and time are considered to only depend on chemistry, not on pressure (low Mach-number approximation). To represent the sub-grid scale stresses and scalar flux, a Smagorinsky model is used along with the dynamic procedure and a constant turbulent Schmidt number of 0.7, a common value used whilst Cook and Riley [17,18] set 0.72. A flamelet approach is used to relate the filtered mixture fraction to density, temperature and species concentrations. The filtered mixture fraction is determined by solving its transport equation, and its sub-grid scale variance is given by an appropriate sub-grid scale model. Thus, the chemical state is defined by the local mixture fraction, the subgrid fluctuation of the mixture fraction and the rate of scalar dissipation. For scalar dissipation, a Delta-function is used to describe its pdf. For modeling, the most basic approach is to describe the rate of scalar dissipation according to its definition.

The equations of continuity, momentum and mixture fraction were transformed into cylindrical coordinates and discretized in space by finite volumes utilizing central schemes. The accuracy of approximation is 4th order for convective terms and 2nd order otherwise. The equations are integrated in time by a 3rd order low-storage Runge–Kutta method, pressure is determined by solving a Poisson equation derived from the equation of continuity.

2.3. Data evaluation: URANS vs LES

Using LES, the averaging is over a scale sufficient to filter small eddies, not resolved by the particular grid being used, but the stochastic nature of turbulent solutions is retained. Hence, Reynolds averaged statistics must be evaluated by accumulating a large enough sample size. In a temporally periodic flow, the samples must be at a fixed phase in order to obtain statistics of the turbulent portion of the flow field. As pointed out in [11] the mesh and time-step requirements of URANS and LES are quite different. Whilst LES resolves the eddies of the turbulence itself, unsteady RANS models the turbulence and resolves only unsteady mean flow structures. Consequently, LES typically requires much higher spatial and temporal resolution, and is more costly. It also requires very long integration time to build an ensemble averaged solution. In order to accurately capture the unsteadiness in the mean flow using URANS, the averaging period should be much smaller than the time scale of the unsteady mean motion. At the same time, the time period should be orders of magnitude higher than the time scale of the random fluctuations, for the averaging to make sense. Unfortunately, note that many engineering flows do not warrant a time period which meets these conditions simultaneously. This leads to the so-called spectral-gap problem. As discussed by Durbin [3] this is due to a misconception that Reynolds averaging equals temporal averaging. If statistical periodicity is defined via the existence of a narrow peak representing the unsteadiness of the flow in the spectrum there is no need for a spectral gap. The peak can occur right in the midst of the broadband turbulent scales and Reynolds averaging is simply interpreted as ensemble or phase averaging. On the other hand, if the unsteady coherent motion creates a strong disequilibrium, the assumptions underlying standard RANS closures might not be sufficient anymore. In this case it might be necessary to incorporate some kind of spectral information into the model, e.g. by using two-time-scale models as proposed in [13].

3. Configurations, results and discussions

Several U-RANS computations of unsteadiness have been reported in the literature. For review, see [3,12,60]. In the first part of this section, a swirled isothermal flow configuration is investigated using U-RANS and a detailed description of the flow topologies is given in comparison to LES and experimental data. In the second part, two flame configurations that were already investigated by means of (not really satisfactory) RANS-based simulations are chosen. As these flames do not exhibit particular unsteady or periodic phenomena, such as coherent or deterministic structures, combustion LES results are simply presented here. Even though LES of reacting flows has been applied to both premixed and non-premixed combustion, only results of turbulent non-premixed flames configurations are discussed here.

3.1. Swirled isothermal flow configuration: URANS/LES [12]

Swirled flows play an important role in many engineering applications such as modern gas turbines, aero-propulsion systems, etc. With regard to design efforts, by adjusting the swirl intensity it is possible to improve the mixing quality of the flow and to influence or to control physicochemical processes, such as the flame stabilization. The effect of swirling number variation on turbulent transport and mixing processes in swirling recirculating flows has been already investigated (e.g. in [45]). While the enhanced mixing and stabilization of the flame caused by the swirl are desirable features, such flows often exhibit hydrodynamic instabilities called precessing vortex core. For design purposes it is very important to predict such instabilities. This application aims at the demonstration of the performance of the unsteady RANS (U-RANS) method in predicting the precessing vortex core phenomenon. For simplicity, a constant density case is investigated.

Experimental and numerical setup. The experimental setup utilized consists of a movable block type swirler which feeds an annulus from which the air flow enters the measurement section at ambient pressure and temperature. The Reynolds number is computed based on the bulk velocity and bluff-body diameter. Three cases were investigated experimentally in which the (geometrical) swirl number was set to $S = 0.75$. Two cases were selected for this paper which will be referred to as the 30 kW ($Re = 10.000$) and 150 kW ($Re = 42.000$) cases (according to the thermal power for premixed operation of the burner). A coflow of 0.5 $\mathrm{m\,s^{-1}}$ surrounds the swirler device. A sketch of the device is given in Fig. 1. The flow fields measurements used were performed at the Technical University of Darmstadt.

The computational domain was shaped cylindrically being 600 mm long with a diameter of 600 mm. Free slip boundary conditions were applied to the lateral boundaries and a zero gradient outflow condition was set for the face surface. First simulations were performed with the inlet boundary being flush with the swirler exit plane, prescribing experimental data taken at 1 mm above the swirler exit as inlet boundary conditions.

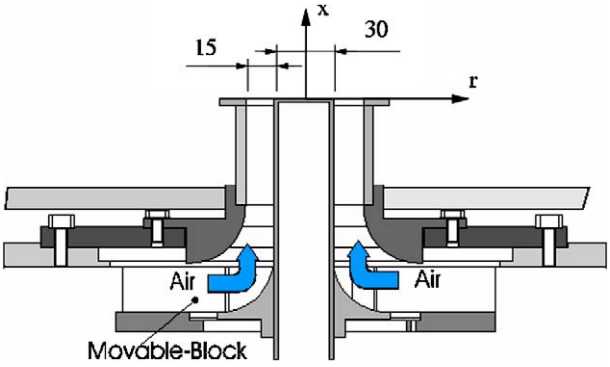

Fig. 1. Sketch of the movable block swirler device and dimensions (in mm). The coordinate system used is attached to the centre of the bluff-body surface.

No instable behavior could be obtained though by doing so. Therefore the swirler device was included in the computational domain. Hence, the inlet boundary was moved to the inlet channels of the swirler device. The swirler was first resolved with 8 cells in the radial direction resulting in a grid with a total of $\approx 500\,000$ cells. After doing so, an unstable behavior of the expected kind was observed in the simulations, but due to unsatisfactory results in the near-nozzle region the resolution of the swirler was then doubled to 16 points in the radial direction. This increased the total number of grid points to $\approx 800\,000$.

Since the swirler device is fed from a plenum chamber, a constant radial inflow velocity was set on the inlet boundary which was adjusted to result in the correct mass flow for the two cases.

Results and discussion: Flow structure. Due to the single-point nature of the LDV technique, no information about instantaneous flow structures could be obtained from the experimental data. This kind of information can be obtained from the LES computations. Fig. 2 shows instantaneous snapshots from the LES flow field covering one revolution of the precessing vortex core. The flow features that can be observed are:

(1) The central reverse flow zone performs a precession motion around the bluff-body of the swirler device.
(2) The recirculation reaches upstream into the swirler device. This explains why the first simulations performed without the swirler failed to predict any unsteady behavior of the flow.
(3) Two opposed helical vortices shed off the outside edge of the swirler exit. They rotate with the same frequency as the recirculation bubble.

As is shown by Fig. 3, the U-RANS clearly captures the precessing vortex core: a rotating movement of the vortex centre about the system's geometrical axis can be observed. It is noteworthy that no converged stationary solution could be obtained which also indicates the unsteady nature of the flow under consideration. When comparing the U-RANS results to phase averaged LES data both methods show the same qualitative overall flow behavior (not shown).

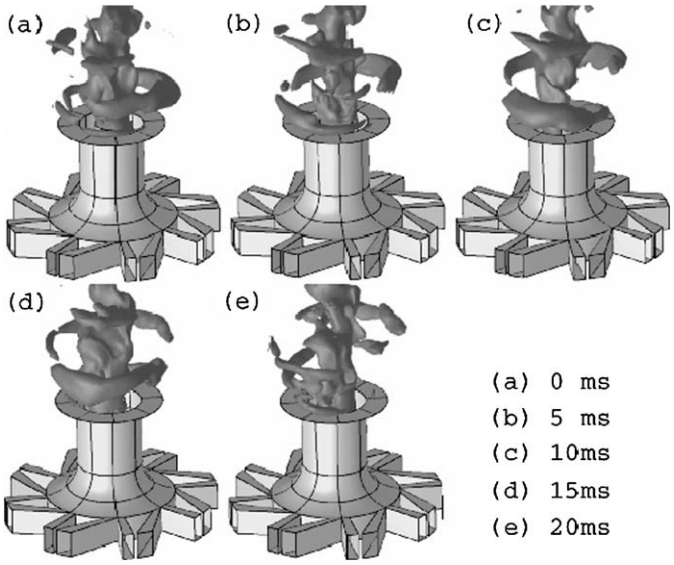

Fig. 2. Isosurfaces of instantaneous axial velocity $u = -0.5\ \mathrm{m\,s^{-1}}$ taken from the LES of case 30 kW showing the flow structure covering one revolution of the vortex core.

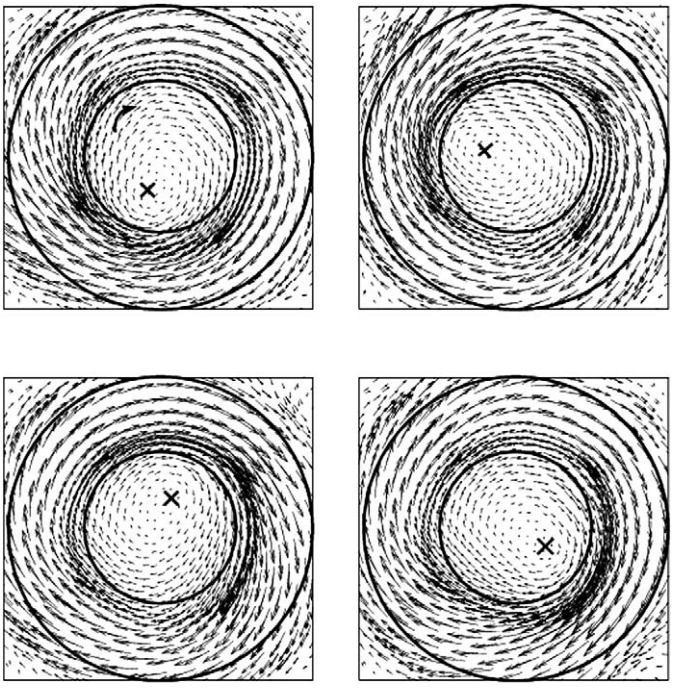

Fig. 3. Sequence of snapshots (top left to bottom right) taken from the U-RANS of the 30 kW case showing vector plots of velocity in a plane $x = 30$ mm. The swirler annulus is indicated by the two concentric circles. The approximate instantaneous vortex centre and precession direction are also indicated.

Velocity and fluctuation profiles. Radial profiles of time averaged axial and azimuthal velocity as well as the turbulent kinetic energy for case 30 kW are shown in Figs. 4–6. Both the LES and the U-RANS simulations capture the experimental mean velocity profiles quite well. Near the swirler exit the DSM gives even better results than the LES. Since the DSM includes a wall-model it has got an advantage in predicting the wall-dominated flow in the swirler device. The unsatisfactory

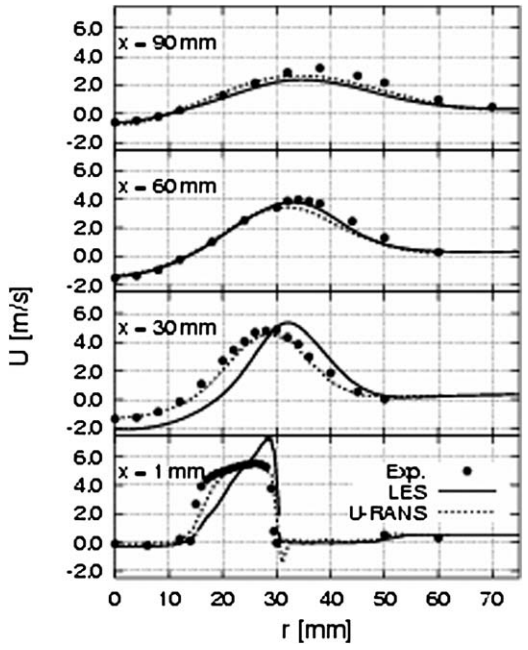

Fig. 4. Radial profiles of time axial velocity at several axial positions (30 kW case).

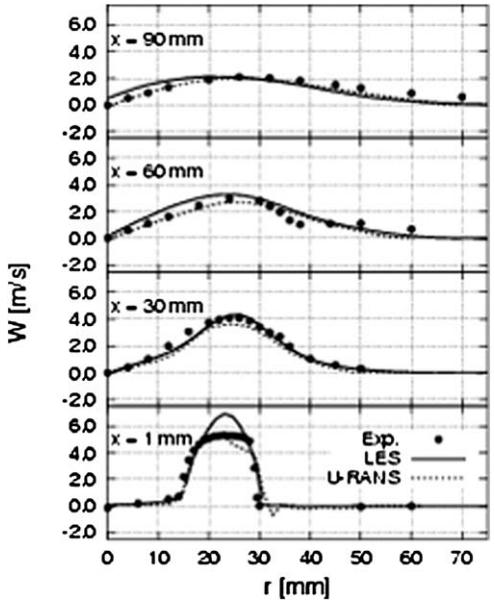

Fig. 5. Radial profiles of time azimuthal velocity at several axial positions (30 kW case).

accuracy of the LES results at the swirler exit can be explained by the relatively coarse grid resolution in the swirler device. Only 16 cells were used to resolve the radial direction of the annulus. This is by far not fine enough for the LES to cover the near wall behavior of the flow. The plots of kinetic energy support this as the peak fluctuations at the swirler exit are located in the annulus middle. Due to the wall-induced shear there should be fluctuation peaks near the wall. In order to overcome this problem, more LES computations would be necessary performed with an increased resolution in the swirler.

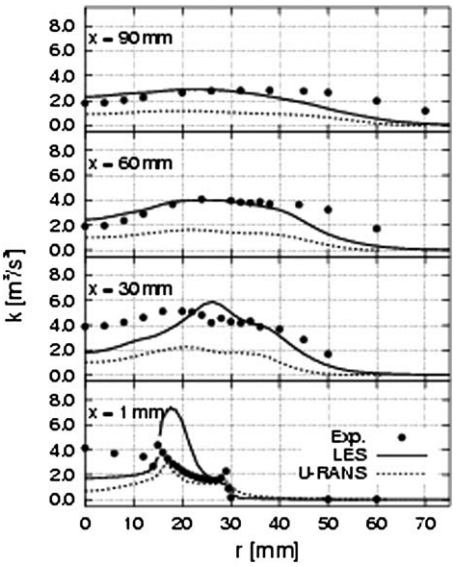

Fig. 6. Radial profiles of time averaged total kinetic energy at several axial positions (30 kW case).

Though the shape of the profiles obtained with the U-RANS for the total kinetic energy in Fig. 6 is quite good, the level of energy is much too low when compared to the experiments. This was found to be much worse in the first computations with lower flux-blending parameters, indicating a significant influence of numerics on the U-RANS results. The LES gives the same level of kinetic energy as the experiments and also captures a good deal of the profile shapes. In the U-RANS framework, kinetic energy denotes the sum of the modeled turbulent kinetic energy and the resolved energy contained in the unsteady flow motion. When comparing velocity time series from the U-RANS to phase averaged time series from the LES, it was found that the amplitude of the coherent velocity fluctuation was much too low in the U-RANS. Hence, the resolved energy is underpredicted by the unsteady RANS. The length and width of the recirculation zone is quite well-predicted by the U-RANS, as the plots of axial velocity indicate in Fig. 4.

Precession frequency. For both the experiment and the LES, the vortex core precession frequency was obtained from the turbulence energy spectrum as computed from temporal autocorrelations (see Fig. 7 (left)). This kind of temporal 2-time turbulent energy spectrum is a non-broad one for the U-RANS (see Fig. 7 (right)), while a spatial two-point information is not available for U-RANS. As can be seen in Fig. 7 the spectra show distinct peaks associated with the motion of the vortex core. Furthermore, these spectra show a second weaker peak at about the doubled PVC frequency. This peak is associated with the opposed helical vortices that are shown by the LES, and more distinctly by U-RANS. Since these helical vortices perform a rotating motion at the same speed as the central recirculation, the monitoring point (at which the velocity time series for the spectral analysis was sampled) is passed twice by such a structure in one PVC cycle. Hence the doubled frequency. As far as the position of the peak frequency in the turbulent spectrum is concerned, it seems that the coherent motion is associated to rather large frequencies. From the temporal autocorrelations of both the LES, U-RANS and the experiments, a factor of approximately five was estimated between the precession period τ and the integral time scale T. This implies that the coherent and turbulent scales are separated from each other.

The precession frequency can also be expressed in terms of the Strouhal number defined as $St = L/\tau.U$, where τ is the inverse of the peak frequency and the characteristic velocity U and length L are the same as were used for computing the Reynolds number. In Fig. 8, the Strouhal numbers corresponding to the peak frequency for the two cases are plotted as a function of Reynolds number.

For a given flow configuration the Strouhal number is expected to reach an asymptotic value in the limit of high Reynolds numbers. The precession frequency then increases linearly with the flow rate. This behavior seems to be correctly captured by the U-RANS. It can be seen that the frequencies obtained from the LES are about 20% higher than those from U-RANS and experiments. This is clearly related to the inexact prediction of velocity profiles in the swirler annulus. In the

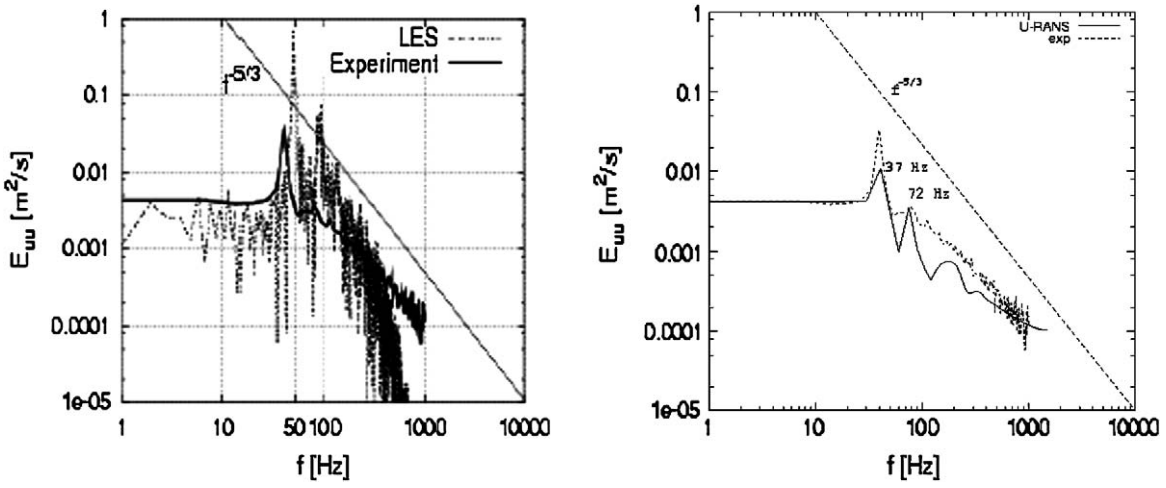

Fig. 7. Turbulent energy spectra computed from temporal autocorrelations at $x = 1$ mm, $r = 20$ mm obtained from the experiments, LES (left) and URANS (right) of the 30 kW case. The dotted line indicates the $f - 5/3$ decay of energy.

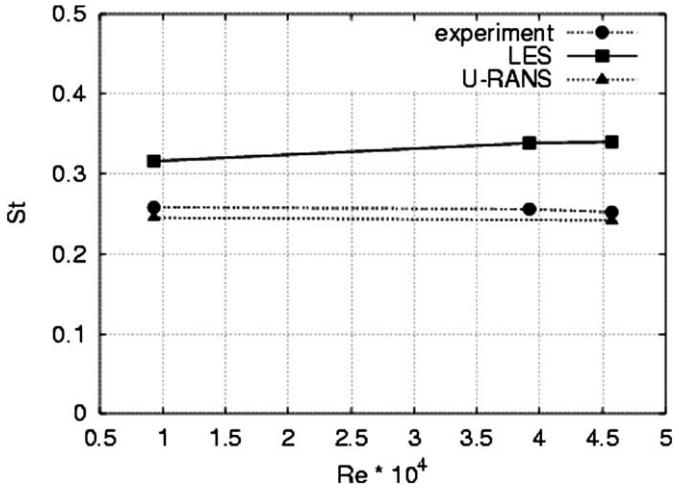

Fig. 8. Dimensionless peak precessing vortex core frequency plotted over Reynolds number.

plots of mean tangential velocity (Fig. 5), at $x = 1$ mm one can see that the LES over-predicts the tangential velocity component. When computing the effective swirl number it was found that in the LES it is about 10–15% higher than in the experiment. This in turn is likely responsible for the over-prediction of the precession frequency which is a function of the swirl number.

So far it could be confirmed that the U-RANS method employing a full Reynolds stress model is able to capture the precessing vortex core phenomenon both qualitatively and in parts also quantitatively. Although a remarkable accuracy was achieved in predicting the vortex core precession frequency, the energy contained in the coherent motion of the PVC was significantly underpredicted by the unsteady RANS. The reason for this is not clear yet, but the amount of numerical dissipation contained in the discretization scheme seems to play an important role.

Furthermore, although it is justified to speak of at least a weak scale separation in the flow considered here, it might still be necessary to take into account disequilibrium effects as discussed above. This is an issue requiring further investigation.

It should be mentioned that for 3-D time dependent simulations as performed in the present study the computational cost is significantly increased when compared to steady state RANS computations. Computational requirements are still low when compared with those for LES. To perform a more accurate LES, a finer mesh should be used in the wall-dominated swirler device. So far LES is very good for flow governed by large, turbulent structures, which can be captured by a fairly coarse mesh. However, if attached boundary layers are important, LES gives partially dissatisfying predictions. Apart from an appropriate near-wall SGS-modeling to get around this bottleneck of LES near walls, many researchers suggest hybrid LES-RANS methods, in which RANS is used near the wall while LES is utilized in the remaining part of the domain. However, the interface coupling remains the main point of issue [3,54].

3.2. A highly turbulent methane flame (standard DLR-flame) [20,31]

Experimental investigation of this configuration has been performed by DLR and Sandia Labs for species fields and EKT (Technical University of Darmstadt) for velocity fields providing complete experimental data sets useful for verification and improvement of mathematical models. It was observed that this flame does not exhibit particular unsteady coherent or deterministic structures. Some interesting PDF/RANS results (see in [31] and therein references) are available, so that additional U-RANS calculations are not found to be necessary. Therefore we simply rely upon combustion LES for its capability of better predicting flow and combustion fields. The precision of the LES results is evaluated by a comparison with experimental data.

Experimental and numerical setup. This flame consists in a fuel mixture of methane (33.2% vol.), hydrogen (22.1% vol.) and nitrogen (44.7% vol.) and achieves a non-lifted methane flame with a stoichiometric mixture fraction of 0.167. Methane was used as a fuel component in order to study the interaction of its well-known chemistry with turbulent flow. Hydrogen was added to stabilize the flame, without changing the simple flow field of the round jet; the dilution by nitrogen was used to decrease thermal radiation and to improve the signal quality of the spontaneous Raman scattering technique employed in experiments [31]. A central nozzle (8 mm of nozzle-diameter) spends the fuel, while a surrounding air coflow is necessary for experimental reasons. The fuel streams of the feeding pipe at a Reynolds-number of 15 200, which corresponds to a bulk velocity of 42.2 m s^{-1}. The laminar air-coflow streams at a rate of only 0.3 m s^{-1}.

We apply LES to this flame and examine its suitability for the simulation. To this end, a cylindric computational domain of 0.38 m length and 0.48 m in diameter was chosen, just beginning at the exit plane of the nozzle. The nozzle and the coflow were modeled using an inflow condition on the abutting face of the cylinder as above. To describe the turbulent inflow, a turbulent velocity profile computed by a preceding LES of a pipe-flow was applied.

The computational domain was discretized with an axisymmetric grid of $129 \times 32 \times 60$ (axial, tangential, radial) cells. To check if this grid resolution was fine enough, the flowfield at the nozzle was recomputed again with refined cells on a domain of half the previous size ($257 \times 32 \times 60$ cells). The computation in the small domain will be labeled C2 (see Figs. 9–12). Assuming the highest velocity and mixture gradients to appear close to the nozzle, this method is capable to check for "grid-independence" without the need for twice as many cells in each direction (i.e. 16 times more CPU-time, approx. 5 months on Alpha 21264). This study shows that an almost grid-independent solution had been achieved, although it shall be stressed here that it is not possible to define a classical grid-independence using the Schumann-filtering since the subgrid model varies with varying filter widths (i.e. cell-size). With smaller resolved length scales, the modeled part of the turbulence vanishes when Kolmogorov-scales are resolved. Fur-

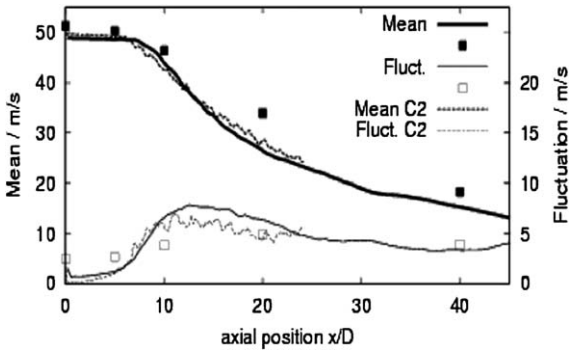

(a)

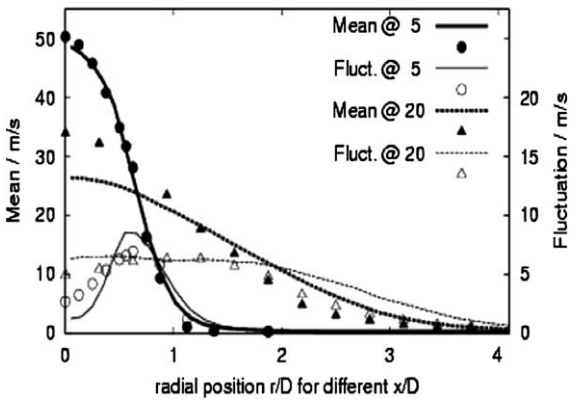

(b)

Fig. 9. Axial velocities over axis/radius.

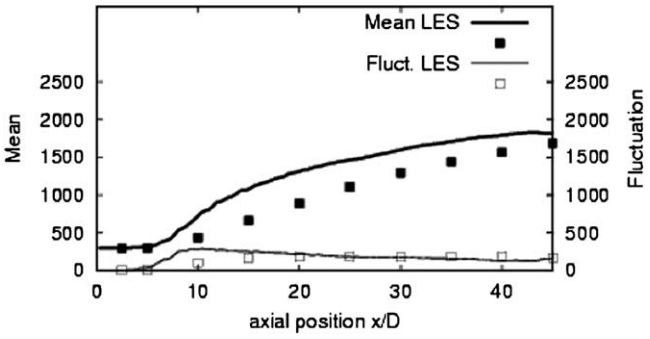

(a)

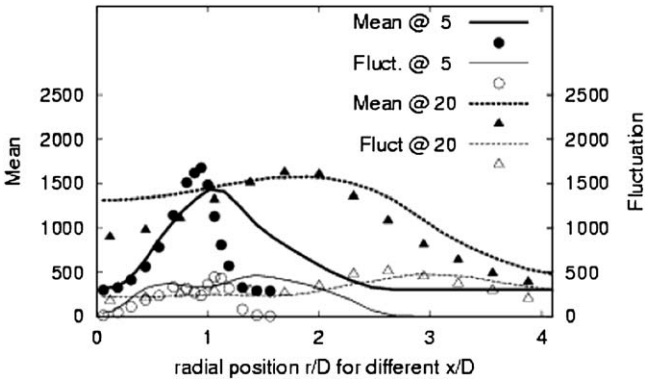

(b)

Fig. 11. Temperature over axis/radius.

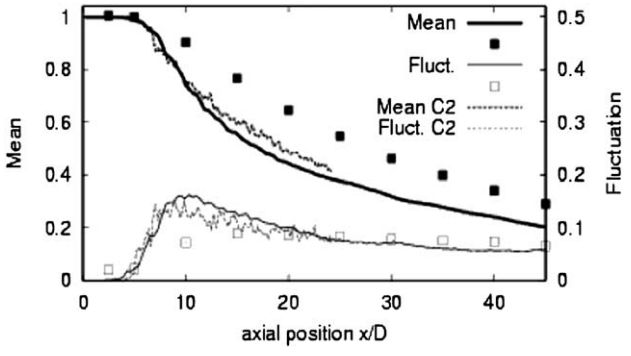

(a)

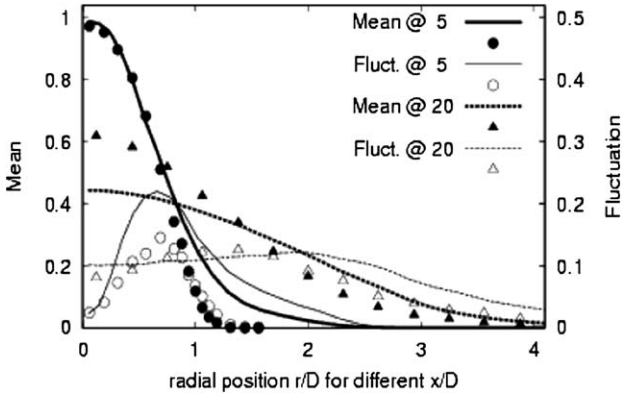

(b)

Fig. 10. Mixture fraction over axis/radius.

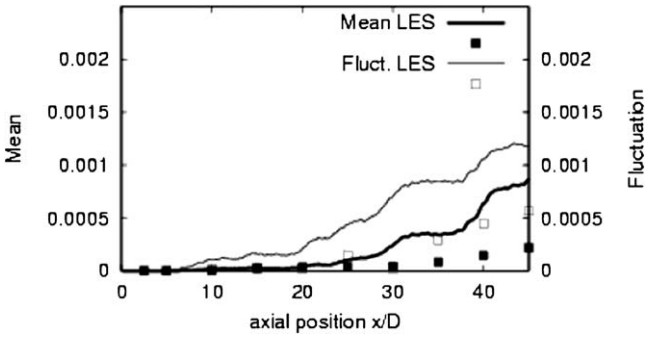

(a)

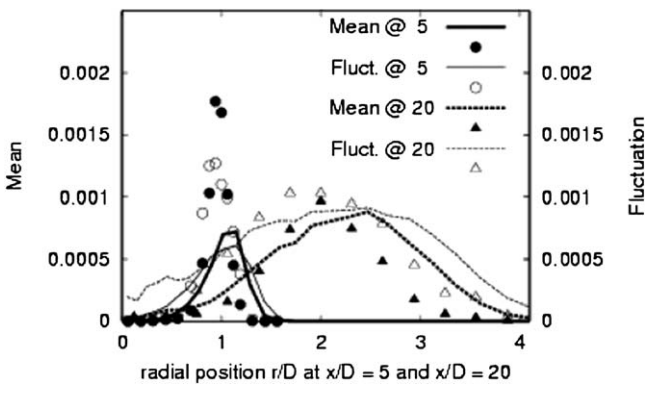

(b)

Fig. 12. OH-Concentration over axis/radius.

thermore, the over-all error from the model will diminish with finer resolution. Accordingly, improved predictions should result with finer grids.

Results and discussion. For the velocity and scalar fields, axial and radial profiles of both mean and standard deviation are shown. For the numerical results, mean values are represented with a fat line, the fluctuation with a fine line of corresponding type. For experimental data, a full symbol is used for the mean values, while the same, empty symbol denotes the fluctuation.

Although experimental and numerical results in Figs. 9–12 generally agree, it is interesting to see how turbulence develops just downstream the nozzle and influences the mixture fraction distribution. The experiments show that the turbulence level in the nozzle is to be expected around 5%, whereas the simulation predicts a far smaller level. The essential features of the turbulence production in the shear layer is well reproduced. The differences observed may be due to inflow-conditions and to reasonably resolving the high gradients (mixture fraction in particular) right at the nozzle. This well-known problem in the literature is connected to the transition from the wall-affected turbulence in the nozzle to the free turbulence, along with a structural change in the turbulence. With RANS modeling, some corrections are generally considered, with regard to the determination of appropriate model parameters. This kind of ad hoc parameter adjustment does not exist in LES using Germano procedure. However, the use of advanced subgrid scale models is then recommended.

All in all, the prediction of the mixing field is satisfying, although the results suffer of inaccuracies in the nozzle-area due to the inaccuracy on flow field in this region. Here, evidence is stronger that the jet breaks up too early, resulting in a strong decay of the mixture fraction along the axis. This is confirmed by Fig. 10(b), which shows too lean mixture at the axis and too rich mixture away from it. Here again, it is interesting to study the axial development of the fluctuation. The predicted curve starts at zero, which corresponds to the jet potential core. At 5 diameters downstream, the jet suddenly breaks up with very high fluctuations. Further downstream, where gradients in the mixture fraction have been smoothed, the prediction of the fluctuation agrees well with the experimental data. That from the computation the jet breaks up too early is not really astounding since study of jet break up requires a very high grid resolution to reasonably resolve the gradients in the mixture fraction field. Errors in the mixing field (mean and fluctuation) certainly impinge the density fields and thus influence the velocity field as well.

As one would expect, the temperature in Fig. 11 behaves similar to the mixture fraction, with high temperatures being predicted too early (i.e. too far upstream). Since there is a strong non-linear relation between temperature (or density) and mixture fraction, the error in the prediction of the mixture fraction appears amplified here. This is mainly true for the radial profile of the mean temperature at $x/D = 5$, at a radial position of $r/d = 1.5$. There, a temperature of 1000 K is predicted, while measurements show that this area is not affected by chemical reaction yet. However, the temperature at the location ($x/D = 5$; $r/D = 0.9$) is slightly underpredicted. Further downstream, away from the nozzle-area, the results look much better again, but certainly, they still rely on the predictions at the nozzle. Therefore, a good predictability depends strongly on an appropriate choice of boundary and inflow conditions. This issue is accounted for in the next application by considering a digital filter based generation of inflow data [42].

Since the main species are defined by the mixture fraction, they all behave similar and thus do not need to be presented. However, flamelet chemistry introduces some interesting information on minor species, so that OH-concentration shall be given here (Fig. 12). At $x/D = 5$, OH-concentration is completely underpredicted. This corresponds to the low temperatures in this area, which have been described above. At the position $x/D = 20$, the predicted OH-concentrations agree well with experimental measurements.

3.3. Turbulent piloted methane/air diffusion flame: (Sandia) flame D

This configuration is especially chosen in order to show how LES can be used to provide comprehensive information of a flame, such as structure of the flame in terms of lengthscales and scalar dissipation rate. There were many numerical simulations of flame D, often contributed to the workshop on turbulent non-premixed flames (TNF) [41], but not containing such kind of information. The turbulent flow was modeled by RANS, PDF-methods, one-dimensional turbulence, as well as LES. The mixing was described by different RANS-models, via PDF-methods and also with LES. Finally, the chemical state was determined by full or reduced reaction mechanisms, by Intrinsic Low-Dimensional Manifolds (ILDM), by conditioned moment closure (CMC), steady or unsteady flamelets or with an equilibrium assumption. Flame D may well be the best-investigated turbulent flame, which turns it into the ideal benchmark for modeling approaches.

Experimental and numerical setup. The burner investigated was designed at Sydney University. Scalar data was obtained by Raman/Rayleigh/LIF measurements at Sandia National Laboratories. Velocities were measured with Laser Doppler Anemometry (LDA) at Technical University of Darmstadt. The Sydney burner consists of a long fuel-pipe that delivers the methane–air mixture (25/75% vol., $f_{\text{stoic}} = 0.35$) at a Reynolds-number of $Re = 22\,400$ ($u_{\text{jet,bulk}} = 49.6\ \text{m s}^{-1}$, $D = 7.2$ mm). A premixed pilot flame ($u_{\text{pilot,bulk}} = 11.4\ \text{m s}^{-1}$, $D_{\text{pilot}} = 18.2$ mm) provides the heat and radicals to stabilize the jet flame. The pilot flame results in a composition of product species equivalent to a mixture fraction of $f_{\text{pilot}} \approx 0.27$. A coaxial laminar coflow spends air at a rate of $0.9\ \text{m s}^{-1}$.

Two simulations were performed with $1025 \times 32 \times 60 \approx 2.0 \times 10^6$ nodes in axial, circumferential and radial direction. The first simulation was performed in a large domain (70 D in length and 25 D in diameter) to examine the entire flame. The second simulation in a small domain (40 D $\times$ 15 D) achieves a finer resolution and yields better information on scalar lengthscales and rates of scalar dissipation. Consider-

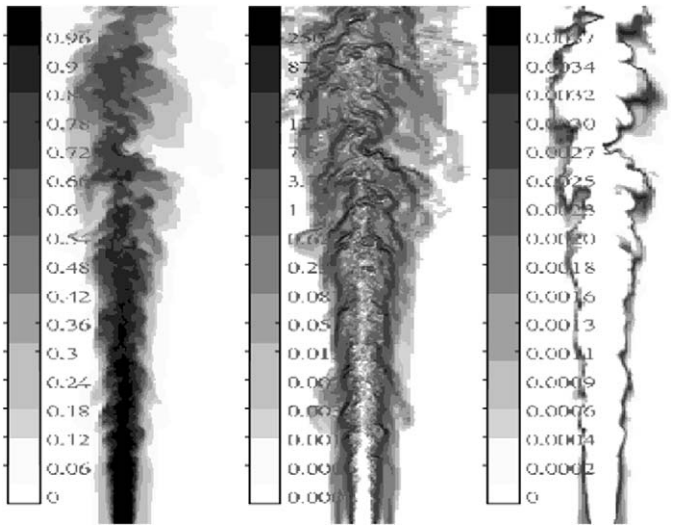

Fig. 13. Instantaneous snapshots of mixture fraction (left), scalar rate of dissipation (middle) and OH mass fraction (right). The fields were obtained from the LES with fine resolution. The domain shown is a section 10 D × 40 D (approx. 75 × 1000 nodes), starting from the exit plane. No interpolation was applied, the scalar rate of dissipation is scaled logarithmically.

ing that the scalars are mainly transported in axial direction (Fig. 13), a very fine grid-spacing was chosen in this direction. The computations were conducted on single processor computers within approximately three weeks (Intel P4, 3.0 GHz, Spec CFP2000: 1200). The inflow plane of the domain was placed two diameters D upstream of the nozzle to improve the prediction of the nozzle-flow. On the inflow plane, experimental mixture fraction and velocity profiles were forced, whereas a zero-gradient condition was applied for pressure. The outflow boundary is modeled with a zero-gradient condition as well, while on the surface of the cylinder a simplified momentum equation allows entrainment (see e.g. [26,27,58]). Transient inflow velocities consist of the mean value with fluctuations superimposed. These fluctuations were obtained from a procedure by Klein et al. [42], Kempf et al. [43], that generates reproducible artificial turbulence on arbitrary grids. This procedure satisfies a given integral lengthscale as well as a given Reynolds-stress tensor. The Reynolds-stresses were extracted from experimental data and the lengthscale L was set according to the simplified mixing length approach $L = C\Delta r$. Therein, Δr is the distance from the closest wall and C is a constant. The value $C = 2/3$ was used.

Results and discussion. The LES computes filtered, time resolved fields of velocity and mixture fraction, that are processed to determine the chemical state. Fig. 13 shows an instantaneous snapshot of the mixture fraction field (left), the scalar rates of dissipation (middle) and the corresponding OH mass fraction (right). These plots provide a good impression of the complex transport phenomena that occur in non-premixed combustion. Since they are not interpolated, they also show the resolution of the grid.

According to [10], the resolved fraction $r_k = k_{\text{res}}/(k_{\text{res}} + k_{\text{sgs}})$ of the turbulent kinetic energy k represents an important parameter to better qualify the LES results.This evolution re-

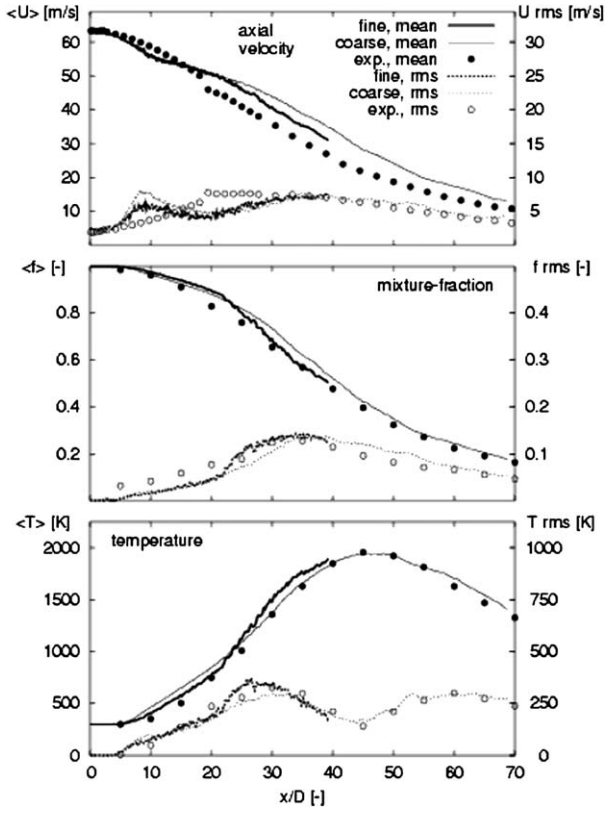

Fig. 14. Profiles of the mean and the standard deviation of axial velocity, mixture fraction and temperature along the centerline.

lies on the modeled expression used, $k_{\text{sgs}} = (\nu_t/C_s\Delta)^2$, with $C_s = 0.1$ and ν_t the turbulent viscosity. This approximation shows that everywhere inside of the domain, more than 73% of the kinetic energy are resolved and only in the region close to the nozzle, r_k drops below 80%.

The mean and standard deviations of various quantities along the centerline are shown in Figs. 14 and 15. In each plot a bold line corresponds to the LES with fine resolution and small domain. The thin line represents the coarse resolution and large domain. The results obtained on the different meshes vary only little, which confirms that the combined error in modeling and discretization of the presented LES is (almost) grid-independent.

In Fig. 14 some overprediction of the mean axial velocity can be observed. The overpredicted velocity-fluctuations (at $x/D \approx 10$) portends to a "nozzle problem", which seems to be related to the hardly resolvable thin mixing and boundary layer at the nozzle. The axial profiles for the mixture fraction are well-predicted, only for $x/D < 20$, the fluctuation is too small. Steiner and Pitsch [26] observe the same and suggest that this might be related to experimental uncertainties. The excellent agreement of temperature mean and standard deviation at different axial positions indicates that the underlying modeling assumptions (mixture fraction approach, equal diffusivity, steady flamelet relation, eddy-diffusivity for scalar rate of dissipation) work very well.

This is confirmed by the well-predicted species mass fractions of OH, H_2O and CO_2, shown in Fig. 15. In contrast, the

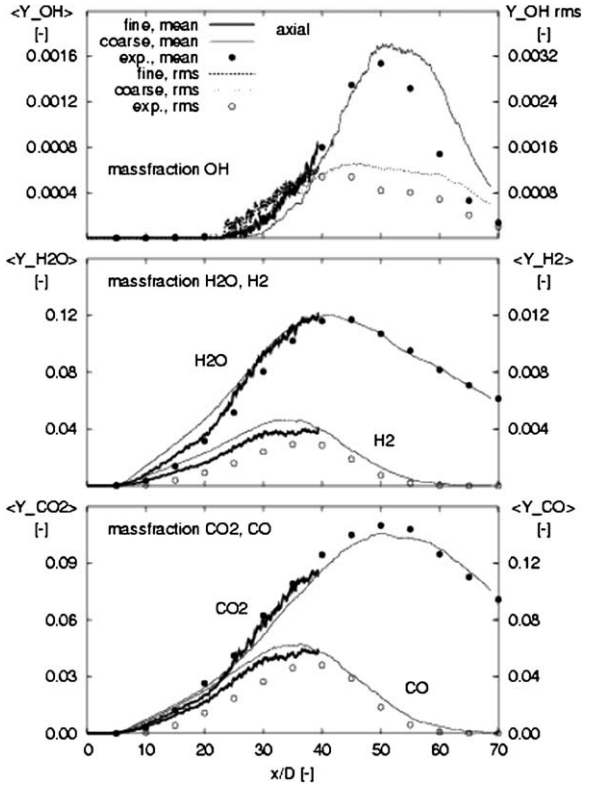

Fig. 15. Profiles of the mean mass fractions of chemical species OH, H_2O, H_2, CO_2 and CO along the centerline. The fluctuations of OH are also shown.

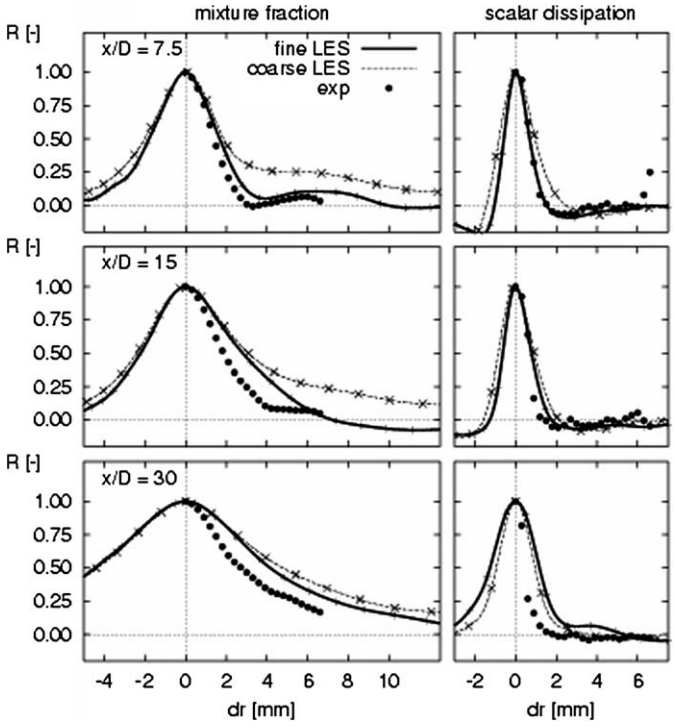

Fig. 16. Spatial autocorrelations of the mixture fraction and scalar rate of dissipation in radial direction at the position of the mean stoichiometric mixture fraction.

intermediate species H_2 and CO are overpredicted in the fuel rich regions ($x/D < 40$), resulting from an overpredicted reaction rate, inherent to the steady flamelet approach [26,27]. Still, the major features (flow, mixing and major species) of the flame are captured well. Corresponding RANS results, except for H_2 and CO, have been obtained in [57] using different first and second order level turbulence models. These results that do not really differ from URANS, because unsteadiness processes are not impressed, seem to be less accurate than the LES results. In particular, further insight to the flame could be achieved by LES.

In fact the spatial autocorrelations in radial direction of the mixture fraction and scalar dissipation at the radius of the mean stoichiometric mixture for $x/D = 7.5, 15, 30$ are shown in Fig. 16. The LES tends to overestimate the lengthscales, which improves on the refined grid. However, the experiment observes that the width of the autocorrelation function for the scalar rate of dissipation decreases in axial direction. In contrast, the LES predicts the opposite behaviour. This might be caused by increasing axial and circumferential components of the mixture fraction gradient in axial direction, that cannot be captured by the experiment, but contribute to the scalar rate of dissipation in the simulation.

4. Conclusions

The results presented in this paper reveal that U-RANS methods could provide an efficient alternative to LES taking into account an adequate turbulence model and sufficient numerical accuracy. It was demonstrated that the most important drawback of LES is the requirement to use very fine grid near walls. The grid must be fine in all directions, not only the wall-normal direction. As U-RANS performs well for predicting unsteady flows, one approach to get around this bottleneck is the hybrid LES-RANS, in which RANS is used near wall while LES is utilized in the remaining part of the domain. Furthermore, the need of simulating complex systems with several parts that have to be computed with different flow solvers requires an exchange of information at the interfaces of the computational domains of each part. Gas turbine systems including multi-component phenomena, such as compressor/combustor instability or combustor/turbine hot-streak migration are typical examples [54]. In the compressor and the turbine part, the flow solver must better account for the moving blades, the wall turbulence, and predict the pressure and density distribution. A such flow solver has to be based on the RANS-approach. In the combustion chamber part, the flow solver has to be able to handle with flows governed by large scale turbulence, chemical reactions, and radiation. This flow solver may be based on LES.

Unfortunately, even the best current LES modeling techniques do not provide reliable and accurate quantitative predictions in complicated flow situations. But models for these and many other flow situations can be developed by formally minimizing the mean square error in the evolution of the resolved field. Given sufficient data from idealized flows, this minimization can be done, resulting in an accurate LES formulation and a measure of the uncertainty (i.e. the mean square error). Further, these techniques can be used to optimize and evaluate any of the

various styles of LES (e.g., no-model, URANS, or classical). For the combustion-LES, prediction results may be improved by using advanced mixing and chemistry models. In some combustion systems, the consideration of two phase flows, liquid spray break up and vaporization brings additional complexities that must be included in advanced unsteady models, in particular in subgrid models for LES [57].

It appears that, there is not one right approach as well recognized in [10]. While the use of LES in engineering applications will certainly increase in the future, the use of URANS models will be prevalent for some specific industry applications [60]. Efforts directed to extend the applicability of LES to complex configurations of technical importance under concevable computing time as well as to continue to improve the performance prediction of existing turbulence modeling approaches must be pursued.

Acknowledgements

The authors gratefully acknowledge the financial support of the DFG.

References

[1] S. Ghosal, P. Moin, The basic equations for the large eddy simulation of turbulent flows in complex geometry, J. Comput. Phys. 118 (1995) 24–37.
[2] P. Moin, Advances in large eddy simulation methodology for complex flows, in: Turbulent Shear Flow Phenomena 2, TSFP2, Stockholm, 2001.
[3] P. Durbin, A perspective on recent developments in RANS modeling, in: W. Rodi, N. Fueyo (Eds.), Engineering Turbulence Modelling and Experiments, vol. 5, Elsevier, Amsterdam, 2002, pp. 3–16.
[4] M. Germano, U. Piomelli, P. Moin, W.H. Cabot, A dynamic subgrid scale eddy viscosity model, Phys. Fluids A 3 (1991) 1760–1765.
[5] M. Lesieur, O. Metais, New trends in large eddy simulation of turbulence, Annu. Rev. Fluid Mech. 28 (1996) 45–82.
[6] P. Sagaut, Large Eddy Simulation for Incompressible Flows, Springer, Berlin, 2001.
[7] C.G. Speziale, Turbulence modeling for time-dependent RANS and VLES: A review, AIAA J. 36 (2) (1998) 173–184.
[8] J.A. Langford, R.D. Moser, Optimal LES formulation for isotropic turbulence, J. Fluid Mech. 398 (1999) 321–346.
[9] C. Meneveau, T. Lund, W. Cabot, A Lagrangian dynamic subgrid-scale model of turbulence, J. Fluid Mech. 319 (1996) 353–385.
[10] S. Pope, Ten questions concerning the large-eddy simulation of turbulent flows, New J. Phys. Focus Issue Turbulence, submitted for publication.
[11] G. Ioccarino, A. Ooi, P.A. Durbin, M. Behnia, Reynolds averaged simulation of unsteady separated flow, Int. J. Heat Fluid Flow 24 (2003) 147–156.
[12] B. Wegner, C. Maltsev, C. Schneider, A. Sadiki, A. Dreizler, J. Janicka, Evaluation of URANS performance in predicting an unconfined swirling flow with precessing vortex core based on LES and experiments, in: Third Int. Symp. on Turbulence and Shear Flow Phenomena, Senai, Japan, 25–27 June, 2003.
[13] K. Hanjalic, B. Launder, R. Schiestel, Multiple time-scale concepts in turbulent transport modelling, in: L. Bradbury, F. Durst, B. Launder, F. Schmidt, J. Whitelaw (Eds.), Turbulent Shear Flows, vol. 2, Springer, Berlin, 1980, pp. 36–49.
[14] K. Hanjalic, Second-moment turbulence closures for CFD: Needs and prospects, IJCFD 12 (1999) 67–97.
[15] U. Schumann, Large eddy simulation of turbulent diffusion with chemical reactions in the convective boundary layer, Atmos. Env. 23 (8) (1989) 1713–1727.
[16] C. Fureby, S.-I. Möller, Large eddy simulation of reacting flows applied to bluff body stabilized flames, AIAA J. 33 (12) (1995) 2339–2347.
[17] A.W. Cook, J.J. Riley, A subgrid model for equilibrium chemistry in turbulent flows, Phys. Fluids A 6 (1994) 2868–2870.
[18] A.W. Cook, J.J. Riley, S.M. de Bruyn Kops, A subgrid scale model for nonpremixed turbulent combustion, in: Proceedings of the Eleventh Symposium on Turbulent Shear Flows, Grenoble, France, 1997.
[19] H. Forkel, J. Janicka, LES of a turbulent hydrogen diffusion flame, in: Flow, Turbulence and Combustion, 2001.
[20] A. Kempf, C. Schneider, A. Sadiki, J. Janicka, LES of a highly turbulent methane flame: Application to the DLR Standard flame, in: TSFP2, Stockholm, 2001, pp. 315–320.
[21] P.J. Colucci, F.A. Jaberi, P. Givi, S.B. Pope, Filtered density function for large eddy simulation of turbulent reacting flows, Phys. Fluids A 10 (1998) 499–515.
[22] M. Düsing, Large eddy Simulation turbulenter Vormischflamme, PhD thesis, TU-Darmstadt, 2004.
[23] D. Veynante, T. Poinsot, LES of combustion instabilities in turbulent premixed burners, in: Annual Research Briefs, 1997.
[24] W.W. Kim, S. Menon, LES of turbulent fuel/air mixing in a swirling combustor, in: AIAA 99-0200, 37th Aerospace Sciences Meeting and Exhibit, 1999.
[25] W.H. Calhoon, S. Menon, Subgrid modeling for reacting large-eddy simulations, in: AIAA 96-0516, 34th Aerospace Sciences Meeting, Reno, NV, January 15–18, 1996, pp. 1–21.
[26] H. Steiner, H. Pitsch, Large-eddy simulation of a turbulent piloted methane/air diffusion flame (Sandia flame D), Phys. Fluids 12 (2000).
[27] H. Pitsch, H. Steiner, Scalar mixing and dissipation rate in large-eddy simulations of nonpremixed combustion, Proc. Combust. Inst. 28 (2000) 35–40.
[28] F. Gao, E. O'Brien, A large eddy simulation scheme for turbulent reactings flows, Phys. Fluids A 5 (1993) 1282–1284.
[29] C.D. Pierce, P. Moin, A dynamic model for subgrid-scale variance and dissipation rate of a conserved scalar, Phys. Fluids 10 (12) (1998).
[30] E.R. Hawkes, R.S. Cant, A flame surface density approach to large eddy simulation of premixed turbulent combustion, Proc. Combust. Inst. 28 (2000) 51–58.
[31] W. Meier, R. Barlow, J.-Y. Chen, Raman/Rayleigh/LIF measurements in a turbulent CH4/H2/N2 jet flame: Experimental techniques and turbulence chemistry interaction, Combust. Flame 123 (2000) 326–343.
[32] C.D. Pierce, P. Moin, Large eddy simulation of a confined coaxial jet with swirl and heat release, AIAA Paper 98-2892, 1998.
[33] W.P. Jones, N. Branley, Large eddy simulation of a turbulent non-premixed flame, in: Proceedings of the Eleventh Symposium on Turbulent Shear Flows, Grenoble, France, 1997.
[34] S.I. Möller, E. Lundgren, C. Fureby, Large eddy simulation of unsteady combustion, Proc. Combust. Inst. 26 (1996) 241–248.
[35] C. Jimenez, C. Dopazo, L. Valino, Application of an Eulerian Monte Carlo field method to the simulation of the filtered PDF in LES, in: C. Dopazo et al. (Eds.), Advances in Turbulence VIII, CIMNE, Barcelona, 2000.
[36] O. Colin, F. Ducros, D. Veynante, T. Poinsot, A thickened flame model for LES of turbulent premixed combustion, Physics of Fluids (1999).
[37] J. Piana, F. Ducros, D. Veynante, LES of turbulent premixed flames based on the G-equation and a flame front wrinkling description, in: Proc. 11th Symp. on Turbulent Shear Flows, Grenoble, France, 1997.
[38] A. Maltsev, A.. Sadiki, J. Janicka, Coupling of extended BML model and advanced turbulence and mixing models in predicting partially premixed flames, in: Third Int. Symp. on Turbulence and Shear Flow Phenomena, Senai, Japan, 25–27 June, 2003.
[39] H. Pitsch, L. Duchamp de Lageneste, Large-eddy simulation of premixed turbulent combustion using a level-set approach, in: Proceedings of the Combustion Institute 29, 2001–2008, Sapporo, Japan, 2002.
[40] H. Pitsch, A G-equation formulation for large-eddy simulation of premixed turbulent combustion, Center for Turbulence Research, Annual Research Briefs, Standford, 2002, pp. 3–14.
[41] R. Barlow (Ed.), Proceedings of the TNF Workshops, Sandia National Laboratories, Livermore, CA, http://www.ca.sandia.gov/TNF.
[42] M. Klein, A. Sadiki, J. Janicka, A digital filter based generation of inflow data for spatially developing direct numerical or large eddy simulations, J. Comput. Phys. 186 (2003) 652–665.

[43] A. Kempf, M. Klein, J. Janicka, Efficient generation of initial- and inflow-conditions for transient turbulent flows in arbitrary geometries, Flow, Turbulence and Combustion, submitted for publication.

[44] D. Veynante, T. Poinsot, Reynolds averaged and large eddy simulation modeling for turbulent combustion, in: O. Metais, J. Ferziger (Eds.), New Tools in Turbulence Modeling, Springer, Berlin, 1997, pp. 105–140.

[45] C. Schneider, S. Repp, A. Sadiki, A. Dreizler, J. Janicka, The effect of swirling number variation on turbulent transport and mixing processes in swirling recirculating flows: Experimental and numerical investigations, in: Proceedings of the 2nd Int. Symp. on Turbulent Shear Flow Phenomena, vol. III, Stockholm, Sweden, 2001, pp. 363–368.

[46] L. Vervisch, T. Poinsot, Direct numerical simulation of non-premixed turbulent flames, Annu. Rev. Fluid Mech. 30 (1998) 655–692.

[47] S.B. Pope, The statistical theory of turbulent flames, Philos. Trans. Roy. Soc. London 291 (1979) 529–568.

[48] S. Menon, P.A. McMurtry, A.R. Kerstein, A linear eddy subgrid model for turbulent combustion: Application to premixed combustion, in: B. Galperin, S.A. Orszag (Eds.), Large Eddy Simulation of Complex Engineering and Geophysical Flows, Cambridge University Press, Cambridge, 1993, pp. 287–314.

[49] C. Meneveau, J. Katz, Scale-invariance and turbulence models for large eddy simulation, Annu. Rev. Fluid Mech. 32 (2000) 1–32.

[50] D.K. Lilly, A proposed modification of the Germano subgrid-scale closure method, Phys. Fluids A 4 (3) (1992) 633–635.

[51] A.W. Cook, J.J. Riley, G. Kosaly, A laminar flamelet approach to subgrid-scale chemistry in turbulent flows, Combust. Flame 109 (3) (1997) 332–341.

[52] H. Pitsch, Extended flamelet model for LES of non-premixed combustion, Annual Research Briefs, 2000, Center for Turbulence Research, Stanford University, USA, 2000.

[53] S. Menon, P. McMurtry, A.R. Kerstein, J.-Y. Chen, A new unsteady mixing model to predict NO_x production during rapid mixing in a dual-stage combustor, AIAA Paper No. 29-0233, 1992.

[54] J.U. Schlütter, S. Shankaran, S. Kim, H. Pitsch, J.J. Alonso, Integration of RANS and LES flow solvers: Interface validation, Center for Turbulence Research, Annual Research Briefs, Standford, 2002, pp. 155–166.

[55] A. Maltsev, J. Bertram, A. Sadiki, A. Dreizler, J. Janicka, Numerical and experimental investigation of flame stabilization of a swirled flow in a model GT combustion chamber, in: Combustion Symposium, Chicago, USA, submitted for publication.

[56] M. Germano, From RANS to DNS: Towards a bridging model, in: P.R. Voke, N.D. Sandham, L. Kleiser (Eds.), Direct and Large-Eddy Simulation III, Kluwer Academic, Dordrecht, 1999.

[57] V. Sankaran, S. Menon, LES of spray combustion in compressible high Reynolds number swirling flows, in: Proc. 2nd Symposium on Turbulent Shear Flow Phenomena, III, 2001, pp. 303–308.

[58] A. Kempf, F. Flemming, J. Janicka, Investigation of lengthscales, scalar dissipation, and flame orientation in a piloted diffusion flame by LES, Proc. Combust. Inst. 30 (2005) 557–565.

[59] B. Merci, A. Maltsev, A. Sadiki, J. Janicka, Comparative study of turbulence and chemistry models on simulation results for a methane/air diffusion flame, Proc. Symp. Turbulence Shear Flow Phenomena (3) 2 (2003) 597–602.

[60] K. Hanjalic, Will RANS survive LES? A view of perspectives, J. Fluids Engrg. 127 (2005) 831–839.